CORE
Metadata, citation and similar papers at core.ac.uk
Provided by Repositorio Institucional de la Universidad de Alicante

Title: Thermal-nanoimprint lithography for perylenediimide-based distributed feedback laser fabrication

Author names and affiliations:
A. Retolaza [a,b], A. Juarros [a,b], D. Otaduy [a,b], S. Merino [a,b], V. Navarro-Fuster [c], M. G. Ramírez [c], P. G. Boj [d], J. A. Quintana [d], J. M. Villalvilla [c] and M. A. Díaz-García [c]

[a] CIC microGUNE
Goiru Kalea 9 Polo Innovación Garaia
20500 Arrasate-Mondragón, Spain
Tel +34 943 73 98 05
E-mail addresses: aretolaza@cicmicrogune.es; ajuarros@cicmicrogune.es; dotaduy@cicmicrogune.es; smerino@cicmicrogune.es

[b] IK4-TEKNIKER
Micro and Nano Fabrication Unit
Polo Tecnológico de Eibar
C/Iñaki Goenaga 5
20600 Eibar, Gipuzkoa, Spain
Tel +34 943 20 67 44
E-mail addresses: aritz.retolaza@tekniker.es; aritz.juarros@tekniker.es; deitze.otaduy@tekniker.es; santos.merino@tekniker.es

[c] Dpto. Física Aplicada, Instituto Universitario de Alicante y Unidad Asociada UA-CSIC.
Universidad de Alicante
03080 Alicante
Tel +34 96 590
E-mail addresses: vinafu@gmail.com; ramirez@ua.es; jmvs@ua.es; maria.diaz@ua.es

[d] Dpto. Óptica, Instituto Universitario de Alicante y Unidad Asociada UA-CSIC
Universidad de Alicante
03080 Alicante
Tel +34 96 590
E-mail addresses: p.boj@ua.es; ja.quintana@ua.es;

Corresponding autor:
Aritz Retolaza

Abstract
In the present work thermal nanoimprint lithography of various commercial thermoplastic resists as matrixes for perylenediimides (PDIs) has been studied. This fabrication method reduced the number of fabrication steps, and therefore, the cost of the obtained distributed feedback (DFB) lasers. The optical properties of these devices are analyzed, aiming to optimize their performance.

Thermal-nanoimprint lithography for perylenediimide-based distributed feedback laser fabrication

Aritz Retolaza [a,b,*], Aritz Juarros [a,b], Deitze Otaduy [a,b], Santos Merino [a,b], Víctor Navarro-Fuster [c], Manuel G. Ramirez [c], Pedro G. Boj [d], José A. Quintana [d], José M. Villalvilla [c] and María A. Díaz-García [c]

[a]CIC microGUNE, Goiru Kalea 9 Polo Innovación Garaia, 20500 Arrasate-Mondragón, Spain
[b]*Micro and Nano Fabrication Unit, IK4-Tekniker, Eibar 20600, Spain*
[c]*Dpto. Física Aplicada, Instituto Universitario de Materiales de Alicante y Unidad Asociada UA-CSIC, Universidad de Alicante, 03080 Alicante, Spain.*
[d]*Dpto. Óptica, Instituto Universitario de Materiales de Alicante y Unidad Asociada UA-CSIC, Universidad de Alicante, 03080 Alicante, Spain.*
**Corresponding author e-mail:aritz.retolaza@tekniker.es*

Abstract

In the present work thermal-nanoimprint lithography of various commercial thermoplastic resists as matrixes for perylenediimides (PDIs) has been studied. This fabrication method reduces the number of fabrication steps, and therefore, the cost of the obtained distributed feedback (DFB) lasers. The optical properties of these devices are analyzed, aiming to optimize their performance.

Keywords: thermal-nanoimprint lithography, organic lasers, distributed feedback lasers, perylenediimide derivatives

1.-Introduction

In the past years organic solid-state lasers (OSLs) have been widely studied mainly because organic materials offer various advantages, such as easy processability in the form of thin films, chemical versatility, wavelength tunability and low cost [1,2]. The discovery of stimulated emission in semiconducting polymer films [3,4] opened the possibility of using electrical excitation to pump the lasers and increased the interest in OSLs.

Distributed feedback (DFB) lasers are among the most studied OSL structures [1,2]. DFBs present several advantages, such as easy deposition of the organic film, low threshold and no need of mirrors. In a DFB laser, the refractive index and/or the gain vary periodically along the structure due to the inclusion of a grating in the substrate or in the active film. Light is “Bragg-scattered” in the grating, thus providing feedback along the waveguide, as well as the mechanism to extract the laser light out of the device [1,2]. In a one-dimensional (1D) DFB laser, the wavelength that satisfies the Bragg condition (λ_{Bragg}) given by

$$m \cdot \lambda_{Bragg} = 2 \cdot n_{eff} \cdot \Lambda \quad (1)$$

where m is the order of diffraction, n_{eff} the effective refractive index of the waveguide, and Λ the grating period, constitutes the resonant wavelength in the cavity, which will then be diffracted in the grating in different directions. For second-order DFBs (m = 2 in eq. (1)) light is coupled out of the film in a direction perpendicular to the waveguide film, by first-order diffraction.

Different techniques have been used to fabricate DFB structures. In some of them, relief gratings have been prepared over the substrate by holographic lithography [5,6], electron beam lithography (EBL) [7,8], laser interference lithography [8] or nanoimprint lithography (NIL) [9-11], and then the active film was deposited on top of them by spin-casting [5], spin-coating [6,7,9-11] or horizontal-dipping coating [8]. In other works direct patterning of the DFB structure on the active medium by UV laser interference ablation [12], two photon polymerization [13], or NIL [7,14-16] processes have been performed. Among all these fabrication methods, NIL is one of the most promising technologies due to its high throughput, low-cost and high fidelity pattern transfer [17,18]. NIL techniques have already shown numerous applications in biology, electronics, photonics and magnetic devices [18-21]. Among NIL processes thermal-NIL (T-NIL), room temperature-NIL (RT-NIL), ultraviolet-NIL (UV-NIL) and combined nanoimprint and photolithography (CNP) can be mentioned. T-NIL is the simplest and most standard one used to imprint conventional thermoplastic materials, which are characterized for having a glass transition temperature (T_g), i.e. a temperature at which a transition in the amorphous regions between the glassy and rubbery state occurs. In order to process these materials by T-NIL, they need to be pressed and heated up to 70-90ºC above the T_g, so typical imprinting temperatures are in the range between 100ºC and 300ºC. The application of such high temperatures for imprinting thermoplastics doped with active molecules, often lead to the degradation of the latter ones, which constitutes an important limitation of the method. A possible way to solve that problem is the use of RT-NIL. RT-NIL has been successfully used to directly pattern conventional thermoplastics as well as low-molar mass organic molecules or conjugated polymers [1,18]. However, since the pressure that must be applied is at least one order of magnitude higher than the one used in a conventional T-NIL, and the pattern cavities in the mold cannot be completely filled during the RT process when thermoplastic materials are used, the achievable imprinting depths are generally lower (typically less than 150 nm) and the quality of the transfer is generally poorer [18]. This fabrication method has been employed to obtain DFB devices [22-24], but due to these

problems their performance is often limited, i.e. high laser thresholds, no precise control in the emission wavelength given certain fabrication parameters, poor photostability, etc. In the case of UV-NIL, this technique allows high fidelity pattern transfer and moderate aspect-ratio (A.R.) at low temperatures. However, it is more sophisticated, and consequently more costly than conventional T-NIL, since it needs high quality transparent stamps, usually made of quartz, for curing polymers by UV-flood exposure. Finally, with regards to CNP, it uses a photochemically curing resist as polymer matrix for T-NIL. It allows obtaining the grating at moderate temperatures, by combining UV-flood exposure, annealing and mold release at the same temperature. CNP has been used to produce high performing 2D DFB structures [25-27].

A wide variety of materials have been used to fabricate the active layers of organic DFB lasers [1,2,28,29]. Among them, our research groups have focused in the last years on polystyrene (PS) films doped with perylenediimide derivatives (PDIs) [9,30-36]. The advantage of using polyimides as lasers dyes is that they are photochemically and thermally stable. In particular, those containing perylene units possess high thermal stabilities because of the condensed aromatic perylene rings [37], and the decomposition temperature of PDIs depends on the nature of the substituents attached to the imide N positions [38,39]. In some of our previous works [31-33], the effect of modifying the chemical structure of the PDIs in their spectral, electrochemical and amplified spontaneous emission (ASE) properties when diluted in liquid solutions, as well as in PS films, at various concentrations, was studied. PDIs symmetrically substituted at the imide nitrogen position, such as *N,N'*-di(1-hexylheptyl)perylene-3,4:9,10-tetracarboxylic diimide (PDI-C6) and *N,N'*-di(2,6-diisopropylphenyl)perylene-3,4:9,10-tetracarboxylic diimide (PDI-O) (see chemical structures in Figure 1) showed the best ASE results. So, efficient DFB lasers based on PS films doped with these dyes and with gratings imprinted on the substrate [9,34,36] or directly on the active film [30], were fabricated. Moreover, the influence of the excitation area on the thresholds of DFBs has also been studied [40].

In this work we have prepared 1D second-order DFB lasers based on polymers doped with PDI-C6 and PDI-O, as laser dyes, fabricated by direct T-NIL of the active film, aiming to optimize the polymers used to disperse the PDIs. For that, thermoplastic polymers, such as mr-I7030E or mr-I8030E have been employed as matrix. The use of direct imprinting of the active films reduces the number of fabrication steps, simplifying the overall process to prepare the DFB lasers and consequently their cost. Results are compared to those previously reported, based on PDI-doped PS films [30].

2.-Experimental

2.1. *Materials*

Several materials were used during the development of the work. Depending on their use they can be classified in:

2.1.1. Matrix to disperse the laser dye

Two commercial thermoplastic polymers for NIL were used as matrix: mr-I7030E and mr-I8030E from Micro Resist Technology GmbH. These resists were methacrylate-based polymers containing aromatic compounds in order to improve the plasma etch resistance and the flow behavior [41]. Their T_g values are 60ºC and 115ºC, respectively. Polymer concentration in the mr-I7030E solution is 10% (±2%) and 9.8% (±2%) in the mr-I8030E solution.

2.1.2. Dyes

Two PDI derivatives have been used: PDI-C6 (M_w = 755 g/mol) and PDI-O (M_w = 711 g/mol). They were purchased from LambdaChem and Phiton, respectively, and their purity was higher than 99.5%. The thermal stability of PDI-C6 and PDI-O was analyzed by differential thermal analysis (DTA) and thermogravimetric analysis (TGA) in a TGA/SDTA851e/LF/1600 Mettler Toledo apparatus, in order to ensure that they do not degrade under the high temperature conditions of the T-NIL process. Results showed that the degradation of PDI-C6 and PDI-O started at a temperature of 345ºC and 389ºC, respectively. These values are above the temperatures used in the NIL process for mr-I7030E (130ºC) and mr-I8030E (165ºC), indicating that the PDI derivatives are thermally stable under the conditions used to fabricate the gratings.

2.2. *Stamp*

A 4-inch diameter silicon negative master, i.e., a stamp with the grating area surrounded by elevated area, was fabricated by EBL and posterior RIE processes by Kelvin Nanotechnology Ltd. The grating area of the stamp was 2.5 mm × 2.5 mm, the periodicity 368 nm, with equal line and space, the depth 260 nm and an A.R. around 1.4. The stamp was subsequently treated with a tridecafluoro-(1,1,2,2)-tetra-hydrooctyl-trichlorosilane antiadhesive coating deposited from the vapor phase in a dessicator connected to the vacuum pump (300 mbar, RT, 40 minutes).

2.3. *Nanofabrication processes*

The DFB devices were fabricated by the following steps: First of all, the thermoplastic matrix was mixed with the dye overnight at RT by agitation. The concentrations of the dyes with respect to the thermoplastic matrix were 0.5 wt% and 1 wt% for PDI-C6 and PDI-O, respectively, following the same concentrations used for PS matrix [32]. After that, a film of the dye doped-matrix mixture was spin-coated over a thermally oxidized 4-inch silicon wafer. Film thickness of mr-I7030E and mr-I8030E were varied between 375 nm and 910 nm by changing the spin-coating speed. Then, as can be seen in Figure 2, the active film was directly imprinted by T-NIL in vacuum by applying a pressure of around 20 bars for 15-30 min, and after that, it was cooled down below T_g. Finally, the stamp was manually demolded. The imprinting and demolding parameters used are shown in Table I.

2.4. *Morphological and optical characterization*

The morphological characterization of the DFB gratings was performed by means of optical microscopy (AXIO Imager.A1m, Carl Zeiss), field emission scanning electron microscopy (FE-SEM, ZEISS Ultra Plus) and atomic force microscopy (AFM, NT-MDT Solver PRO). The thickness of the active films was measured by means of both an interferometer coupled to an optical microscope in reference films deposited over transparent SiO_2 substrates and a Dektak 8 surface profiler in films deposited over thermally oxidized substrates.

The ASE properties of the films deposited over substrates without gratings were explored by optical excitation with a frequency-doubled Nd:YAG (YAG-yttrium aluminum garnet) laser (10 ns, 10 Hz) operating at 532 nm, which lies close to the maximum absorbance of PDI derivatives substituted at the N positions [31]. ASE is a process by which spontaneously emitted light is amplified by stimulated emission as it travels down the waveguide [32, 42]. A scheme of the experimental setup can be found elsewhere [43]. The energy of the pulses was varied using neutral density filters. The pump laser beam was expanded, collimated and only the central part was selected in order to ensure uniform intensity. A cylindrical lens and an adjustable slit were then used to shape the beam into a stripe of 3.5 mm × 0.53 mm. The stripe was placed right up to the edge of the film, from where photoluminescence (PL) emission was collected with an Ocean Optics USB2000-UV-VIS fiber spectrometer with 600 grating lines and a resolution in determining the emission linewidth of 1.3 nm. The precision in measuring the emission wavelength was around half of this value. The ASE photostability was determined by studying the time evolution of the ASE intensity,

while the sample was excited in the same region, at constant pump intensity and under ambient conditions. The parameter used to characterize this property has been the same used in previous works from our group [9,31,32], i.e. the photostability halflife ($\tau_{1/2}$), defined as the time (or number of pump pulses) at which the ASE intensity decays to half of its initial value.

The experimental setup to characterize the laser emission properties of the DFB devices differs from the one used to measure ASE only in the geometrical configuration to excite the sample and to collect the emitted light. In particular, the cylindrical lens was replaced by a spherical one, so the beam over the sample (incident at ~ 20º with respect to the normal to the film plane) was shaped into an elliptical spot (instead of a stripe) with a minor axis of 1.1 mm. The emitted light was collected in a direction perpendicular to the film surface by placing the fiber spectrometer at 1 cm from the sample.

3.-Results

The fabrication and characterization of PS/PDI-C6 based DFBs with gratings engraved by T-NIL directly on the active film was previously reported by us [30]. It was shown that the optical properties of the active films were practically not-affected by the thermal treatments, and that they were very similar to those of lasers of the same characteristics but with the gratings engraved on the substrate. In the present work, the study has been extended to other commercial polymers (mr-I7030E and mr-I8030E), used as matrix, and to two PDI compounds (PDI-C6 and PDI-O), used as laser dyes. The interest of using these alternative resists to PS is that they are provided as ready-to-use solutions and they were modified by the provider to give better flow behavior [41]. In the case of the PS used in our previous works, it was provided in solid form and only toluene was added to prepare the solutions.

Results have been organized depending on the matrix of the active film:

3.1. Lasers based on PDI-doped mr-I7030E active films

The PL and ASE properties of films of different thicknesses (375 nm, 510 nm, 800 nm and 910 nm) of mr-I7030E doped with 0.5 wt% of PDI-C6 were studied before imprinting the DFB gratings. The PL and ASE spectra were similar for all of them. As an illustration, those for the 800 nm-thick film are shown in Figure 3a. These spectra are similar to those of PDI-C6-doped PS films, which were previously reported [35]. As for that case, ASE takes place at a wavelength close to the peak of the (0-1) PL. Figure 3b

displays the spectral linewidth, defined as the full width at half of its maximum (FWHM) as a function of pump intensity, for the same film whose spectra are shown in Figure 3a. This type of plots has been used to determine the ASE threshold ($I_{th\text{-}ASE}$) as the excitation intensity at which the FWHM decays to half of its maximum value. The existence of gain results not only in a spectral narrowing at the threshold, but also in a considerable increase of the output intensity, as also shown in Figure 3b. The performance in terms of threshold of the PDI-C6-doped mr-I7030E films was similar to that obtained for the PDI-C6-doped PS ones. In particular, for the mr-I7030E films explored, $I_{th\text{-}ASE}$ was in the range 10-16 kW/cm^2. These values are comparable to those of PDI-C6-doped PS films: 13-15 kW/cm^2 for a range of thickness between 400 and 1000 nm [35].

The ASE wavelength (λ_{ASE}) for the films based on mr-I7030E was around 580 nm, similar to that obtained for PS films [35]. With respect to the ASE linewidth ($FWHM_{ASE}$) measured well above the ASE threshold, which was around 5-6 nm, results were also similar for both the mr-I7030E and the PS films. An ASE property in which differences between mr-I7030E and PS have been found is the photostability. A $\tau_{1/2}$ value of around 25 min was measured for the PDI-C6-doped mr-I7030E films when pumped with an intensity two times above threshold. This value is much lower than that obtained when the matrix was PS, for which halflives of various hundreds of min were obtained [9].

A DFB laser was prepared by using the PDI-C6-doped mr-I7030E film of 800 nm thickness. According to the stamp used (see experimental section), the resulting grating had a periodicity of 368 nm and equal line and space, and a depth of 260 nm. The DFB spectrum obtained has been included in Figure 3a, so it is possible to compare with the ASE spectrum of the film without grating. As observed, laser emission appears at a wavelength (λ_{DFB}) of 565 nm. The DFB threshold ($I_{th\text{-}DFB}$), determined as the intensity at which the output intensity increases drastically, was 8 μJ/pulse. In order to test the possibility of tuning the emission wavelength by film thickness variation [30,34], a DFB device with the 370 nm-thick film was also prepared. As expected, this device emitted at a lower wavelength (λ_{DFB} = 550 nm) and its threshold was higher (13 μJ/pulse), which is explained by the fact λ_{DFB} is in this case farther away from the maximum of the gain spectrum, at which ASE appears. Detailed discussions at this respect can be found in Ref. 34, in which DFBs were fabricated by spin-coating PDI-C6-doped PS active films on patterned SiO_2 substrates. These thresholds are similar to

those obtained with DFB lasers based on PS (instead of mr-I7030E) films doped with PDI-C6, in accordance with previously discussed ASE results.

We also prepared a mr-I7030E-based DFB laser, but doping with PDI-O, instead of with PDI-C6, motivated by the significantly lower ASE and DFB thresholds of PDI-O when it is dispersed in PS films [36]. The DFB laser had the same grating depth and period as the one just described, film thickness was 540 nm and the PDI-O doping concentration 1 wt%. The emission wavelength of this device was λ_{DFB} = 561 nm and its threshold $I_{th\text{-}DFB}$ = 0.9 μJ/pulse. This threshold value is significantly lower than the one of the device based on PDI-C6 (8 μJ/pulse), emitting at a similar λ_{DFB}.

A property in which these mr-I7030E-based DFB lasers differ from those based on PS is the homogeneity of the active film, which plays an important role in the shape of the DFB spectrum. As discussed in detail in Ref. 34, the lack of uniformity can result in the observation of multiple peaks when analyzing DFB spectra with high resolution spectrometers. Note that the spectra shown in Figure 3a were measured with a low-resolution spectrometer since such apparatus is more convenient for threshold determination purposes. In order to clarify this issue, it is useful to explore the influence of changing the area of the excitation beam over the sample on the shape of the high-resolution DFB spectra. Such study has been carried out in the PDI-O-doped mr-I7030E-based DFB laser (see Figure 4a). As observed, for pump spot diameters (D) of 1 mm and higher, the DFB spectra consist of multiple peaks and their intensities vary quite randomly. This is attributed to the lack of uniformity in the film thickness and the grating structure. Even for D = 0.25 mm, two peaks are observed. A single peak could be obtained only when D was 0.15 mm. These results are in contrast with those obtained with lasers based on PDI-C6-doped PS, for which emission at a single peak could be obtained with larger diameters (i.e for $D \sim 1$ mm) [34].

3.2. Lasers based on PDI-doped mr-I8030E active films

As for the mr-I7030E resist, we first studied the PL and ASE properties of mr-I8030E films doped with 0.5wt% of PDI-C6 and a film thickness of 380 nm. Results were approximately the same than those obtained with mr-I7030E.

A DFB laser was then fabricated by engraving a grating on the PDI-C6-doped mr-I8030E film. The emission wavelength and threshold of this device were λ_{DFB} = 548 nm and $I_{th\text{-}DFB}$ = 8 μJ/pulse, which are similar to those obtained for the laser based on a 370 nm-thick film of PDI-C6-doped mr-I7030E (see section 3.1.). Also in this case we

prepared a mr-I8030E-based DFB laser, but doping with PDI-O, instead of with PDI-C6. Film thickness was 540 nm and the PDI-O doping ratio 1 wt%. Laser emission appeared at λ_{DFB} = 559 nm and its threshold was $I_{th\text{-}DFB}$ = 1 μJ/pulse. Also in this case these parameters are in agreement with those obtained with the mr-I7030E resist.

The influence on the shape of the DFB spectrum of changing the size of the excitation beam was also explored for this device. As shown in Figure 4b, single mode emission was obtained even with spot diameters as large as 1.5 mm. This indicates that in this case film thickness uniformity was very good. The lack of homogeneity when using mr-I7030E (Figure 4a) is associated to the fact that this resist starts to suffer from flow defects as imprinted around the lower end of its recommended temperature [44]. In addition, it presents higher pull-off forces in AFM nanoindentation tests as compared to mr-I8030E [44]. These higher forces lead to higher demoulding forces [44] and may be the reason of a worse uniformity on the imprinted nanostructures.

4. Conclusions

High quality PDI-doped mr-I7030E and mr-I8030E DFB devices have been obtained by direct T-NIL imprinting of the active film. This technique reduces the fabrication steps needed to obtain DFB devices, practically not-affecting their optical properties, and it shows clear advantages to obtain low cost DFB devices. PDI-C6-doped mr-I7030E and mr-I8030E resists shows thresholds for laser emission (8-13 μJ/pulse) similar to those obtained with DFB lasers based on PS films doped with PDI-C6. The thresholds are lower (1 μJ/pulse) when the same matrixes are doped with PDI-O. Single mode emission is obtained, in the PDI-O-doped mr-I8030E devices, with spot diameters as large as 1.5 mm. These all data provide good candidate materials for its selection as low-cost visible laser sources and disposable biosensor chips.

5. Acknowledgements

We thank support from the Spanish Government (MINECO) and the European Community (FEDER) through grants MAT2008-06648-C02 and MAT-2011-28167-C02. Manuel G. Ramírez is supported by a CSIC fellowship within the program JAE.

6. References

[1] I.D.W. Samuel, G.A. Turnbull, Organic semiconductor lasers, Chem. Rev. 107 (2007) 1272-1295.

[2] J. Clark, G. Lanzani, Organic photonics for communications, Nat. Photonics 4 (2010) 438-446.
[3] F. Hide, M.A. Díaz-García, B.J. Schwartz, M.R. Andersson, Q. Pei, A.J. Heeger, Semiconducting polymers: a new class of solid-state laser materials, Science 273 (1996) 1833–1836.
[4] N. Tessler, G.J. Denton, R.H. Friend, Lasing from conjugated-polymer microcavities, Nature 382 (1996) 695–697.
[5] M.D. McGehee, M.A. Díaz-García, F. Hide, R. Gupta, E.K. Miller, D. Moses, A.J. Heeger, Semiconducting polymer distributed feedback lasers, Appl. Phys. Lett. 72 (1998) 1536-1538.
[6] G. Heliotis, R. Xia, D.D.C. Bradley, G.A. Turnbull, I.D.W. Samuel, P. Andrew, W.L. Barnes, Blue, surface-emitting, distributed feedback polyfluorene lasers, Appl. Phys. Lett. 83 (2003) 2118-2120.
[7] M. Salerno, G. Gigli, M. Zavelani-Rossi, S. Perissinoto, G. Lanzani, Effects of morphology and optical contrast in organic distributed feedback lasers, Appl. Phys.Lett. 90 (2007) 111110.
[8] S. Klinkhammer, X. Liu, K. Huska, Y. Shen, S. Vanderheiden, S. Valouch, C. Vannahme, S. Bräse, T. Mappes, U. Lemmer, Continuously tunable solution-processed organic semiconductor DFB lasers pumped by laser diode, Opt. Express 20 (2012) 6357-6364.
[9] V. Navarro-Fuster, E.M. Calzado, P.G. Boj, J.A. Quintana, J.M. Villalvilla, M.A. Díaz-García, V. Trabadelo, A. Juarros, A. Retolaza, S. Merino, Highly photostable organic distributed feedback laser emitting at 573 nm, Appl. Phys. Lett. 97 (2010) 171104.
[10] M. Lu, S.S. Choi, U. Irfan, B.T. Cunningham, Plastic distributed feedback laser biosensor, Appl. Phys. Lett. 93 (2008) 111113.
[11] M. Lu, S.S. Choi, C.J. Wagner, J.G. Eden, B.T. Cunningham, Label free biosensor incorporating a replica-molded, vertically emitting distributed feedback laser, Appl. Phys. Lett. 92 (2008) 261502.
[12] H.H. Fang, R. Ding, S.Y. Lu, J. Yang, X.L. Zhang, R. Yang, J. Feng, Q.D. Chen, J.F. Song, H.B. Sun, Distributed feedback lasers based on thiophene/phenylene co-oligomer single crystals, Adv. Func. Mater. 22 (2012), 33-38.
[13] T. Woggon, T. Kleiner, M. Punke and U. Lemmer, Nanostructuring of organic-inorganic hybrid materials for distributed feedback laser resonators by two-photon polymerization, Opt. Express 17 (2009) 2500–2507.
[14] V. Reboud, J. Romero-Vivas, P. Lovera, N. Kehagias, T. Kehoe, G. Redmond, C.M.S. Torres, Lasing in nanoimprinted two-dimensional photonic crystal band-edge lasers, Appl. Phys. Lett. 102 (2013) 073101.
[15] Y. Chen, Z. Li, Z. Zhang, D. Psaltis, A. Scherer, Nanoimprinted circular grating distributed feedback dye laser, Appl. Phys. Lett. 91 (2007) 051109.
[16] E.B. Namdas, M. Tong, P. Ledochowitsch, S.R. Mednick, J.D. Yuen, D. Moses, A.J. Heeger, Adv. Mater. 21 (2009) 799–802.
[17] H. Schift, Nanoimprint lithography: an old story in modern times? A review, J. Vac. Sci. Technol. B26 (2008) 458-480.

[18] L. J. Guo, Nanoimprint lithography: methods and material requirements, Adv. Mater. 19 (2007) 495–513.
[19] L. J. Guo, Recent progress in nanoimprint lithography technology and its applications, J. Phys. D: Appl. Phys. 37 (2004) R123-R141
[20] H. Schift, NaPANIL Library of processes, second ed., published by the NaPANIL-consortium represented by J. Ahopelto, 2012.
[21] V. Reboud, T. Kehoe, J. Romero Vivas, N. Kehagias, M. Zelsmann, F. Alsina, C.M. Sotomayor Torres, Polymer photonic band-gaps fabricated by nanoimprint lithography, Photonic. Nanostruct. 10 (2012) 632-635.
[22] E. Mele, A. Camposeo, R. Stabile, P. Del Carro, F. Di Benedetto, L. Persano, R. Cingolani, D. Pisignano, Polymeric distributed feedback lasers by room-temperature nanoimprint lithography, Appl. Phys. Lett. 89 (2006) 131109.
[23] D. Pisignano, L. Persano, P. Visconti, R. Cingolani, G. Gigli, G. Barbarella, L. Favaretto, Oligomer-based organic distributed feedback lasers by room-temperature nanoimprint lithography, Appl. Phys. Lett. 83 (2003) 2545-2547.
[24] P. Del Carro, A. Camposeo, R. Stabile, E. Mele, L. Persano, R. Cingolani, D. Pisignano, Near-infrared imprinted distributed feedback lasers, Appl. Phys. Lett. 89 (2006) 201105.
[25] U. Plachetka, A. Kristensen, S. Scheerlinck, J. Huskens, N. Koo, H. Kurz, Fabrication of photonic components by nanoimprint technology within ePIXnet, Microelectron. Eng. 85 (2008) 886-889.
[26] M.B. Christiansen, T. Buß, C.L.C. Smith, S.R. Petersen, M.M. Jørgensen, A. Kristensen, Single mode dye-doped polymer photonic crystal lasers, J. Micromech. Microeng. 20 (2010) 115025.
[27] M.M. Jørgensen, S.R. Petersen, M.B. Christiansen, T. Buß, C.L.C. Smith, A. Kristensen, Influence of index contrast in two dimensional photonic crystal lasers, Appl. Phys. Lett. 96 (2010) 231115.
[28] N. Tessler, Laser based on semiconducting organic materials, Adv. Mater. 11 (1999) 363-370.
[29] M.D. McGehee, A.J. Heeger, Semiconducting (conjugated) polymers as materials for solid-state lasers, Adv. Mater. 12 (2000) 1655-1668.
[30] M.G. Ramirez, P.G. Boj, V. Navarro-Fuster, I. Vragovic, J.M. Villalvilla, I. Alonso, V. Trabadelo, S. Merino, M.A. Díaz-García, Efficient organic distributed feedback lasers with imprinted active films, Opt. Express 19 (2011) 22443-22454.
[31] E.M. Calzado, J.M. Villalvilla, P.G. Boj, J.A. Quintana, R. Gómez, J.L. Segura, M.A. Díaz-García, Effect of structural modifications in the spectral and laser properties of perylenediimide derivatives, J. Phys. Chem. C111 (2007) 13595-13605.
[32] E.M. Calzado, J.M. Villalvilla, P.G. Boj, J.A. Quintana, R. Gómez, J.L. Segura, M.A. Díaz-García, Amplified spontaneous emission in polymer films doped with a perylenediimide derivative, Appl. Optics 46 (2007) 3836-3842.
[33] M.A. Díaz-García, E. M. Calzado, J.M Villavilla, P.G. Boj, J.A. Quintana, F.J. Céspedes-Guirao, F. Fernández-Lázaro, A. Sastre-Santos, Effect of structural modifications in the laser properties of polymer films doped with perylenebisimide derivatives, Synthetic Met. 159 (2009) 2293-2295.

[34] V. Navarro-Fuster, I. Vragovic, E.M. Calzado, P.G. Boj, J.A. Quintana, J.M. Villalvilla, A. Retolaza, A. Juarros, D. Otaduy, S. Merino, M.A. Díaz-García, Film thickness and grating depth variation in organic second-order distributed feedback lasers, J. Appl. Phys. 112 (2012) 043104.
[35] E.M. Calzado, M.G. Ramírez, P.G. Boj, M.A. Díaz-García, Thickness dependence of amplified spontaneous emission in low-absorbing organic waveguides, Appl. Optics 51 (2012) 3287-3293.
[36] M.G. Ramírez, M. Morales-Vidal, V. Navarro-Fuster, P.G. Boj, J.A. Quintana, J.M. Villalvilla, A. Retolaza, S. Merino, M.A. Díaz-García, Improved performance of perylenediimide-based lasers, J. Mater. Chem. C1 (2013) 1182-1191.
[37] M.D. Damaceanu, S. Chisca, P.C. Constantin, M. Bruma, High performance perylenediimide-based copolymers and thin films made therefrom, Proceedings of the international conference "Nanomaterials: applications and properties" 1 (2012) 01NDLCN09
[38] Y. Nagao, Synthesis and properties of perylene pigments, Prog. Org. Coat. 31, (1997) 43-49.
[39] G. Turkmen, E.E. Sule, S. Icli, Highly soluble perylene dyes: Synthesis, photophysical and electrochemical characterization. Dyes and Pigments, 83 (2009) 297-303.
[40] E.M. Calzado, J.M. Villalvilla, P.G. Boj, J.A. Quintana, V. Navarro-Fuster, A. Retolaza, S. Merino, M.A. Díaz-García, Influence of the excitation area on the thresholds of organic second-order distributed feedback lasers, Appl. Phys. Lett. 101 (2012) 223303.
[41]http://www.microresist.de/products/polymers_nil/pdf/pi_mri_7te_8te_en_07062201_ls_neu.pdf
[42] M.D. McGehee, R. Gupta, S. Veenstra, E.K. Miller, M.A. Díaz-García, A.J. Heeger, Amplified spontaneous emission from photopumped films of a conjugated polymer, Phys. Rev. B 58 (1998) 7035-7039.
[43] M.A. Díaz-García, E.M. Calzado, J.M. Villavilla, P.G. Boj, J.A. Quintana, F. Giacalone, J.L. Segura, N. Martín, Concentration dependence of amplified spontaneous emission in two oligo-(p-phenylenevinylene) derivatives, J. Appl. Phys. 97 (2005) 063522.
[44] H. Atasoy, M. Vogler, T. Haatainen, A. Schleunitz, D. Jarzabek, H. Schift, F. Reuther, G. Gruetzner, Z. Rymuza, Novel thermoplastic polymers with improved release properties for thermal NIL, Microelectron. Eng. 88 (2011) 1902-1905.

Table I. Parameters for direct imprinting of thermoplastic resist-based active films (T: temperature; t: time).

MATRIX	T imprinting (ºC)	t imprinting (min)	T demolding (ºC)
mr-I7030E	130	25	50
mr-I8030E	165	30	80

Figure Captions

Figure 1. Chemical structures of PDI-C6 (a) and PDI-O (b).

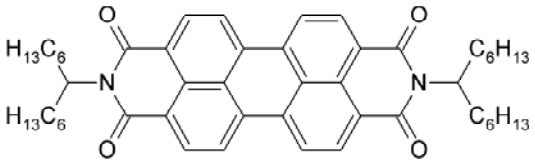

(a)

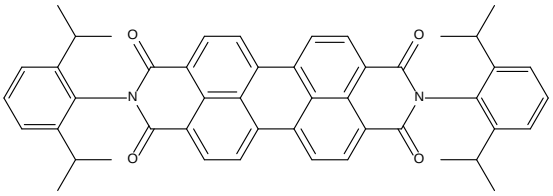

(b)

Figure 2. Scheme of the DFB laser fabrication, based on T-NIL process.

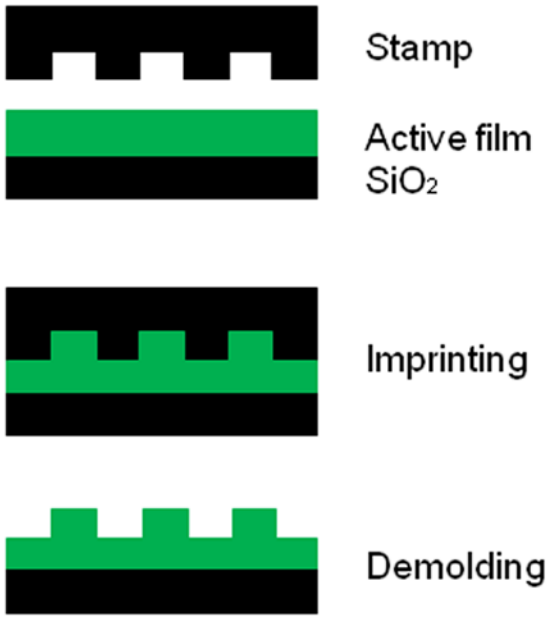

Figure 3. (a) Emission spectrum of a DFB laser based on a 800 nm-thick film of mr-I7030E doped with 0.5 wt% of PDI-C6. The PL and ASE spectra collected from a region without grating is also included; (b) Output intensity at λ = 579 nm (left axis, open symbols) and linewidth, FWHM (right axis, full symbols), as a function of pump intensity collected from a region without grating

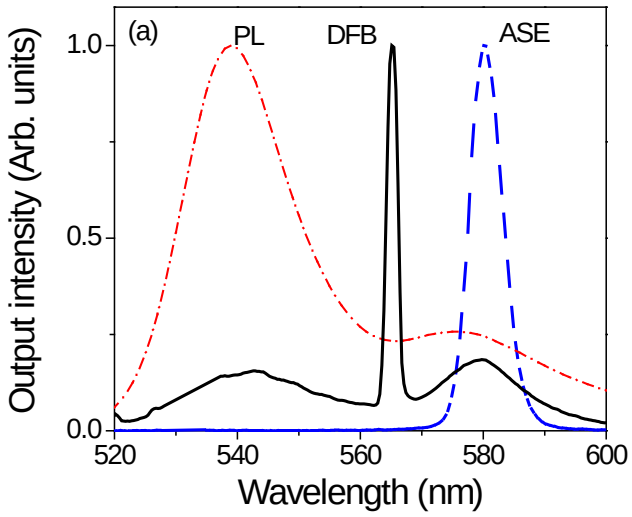

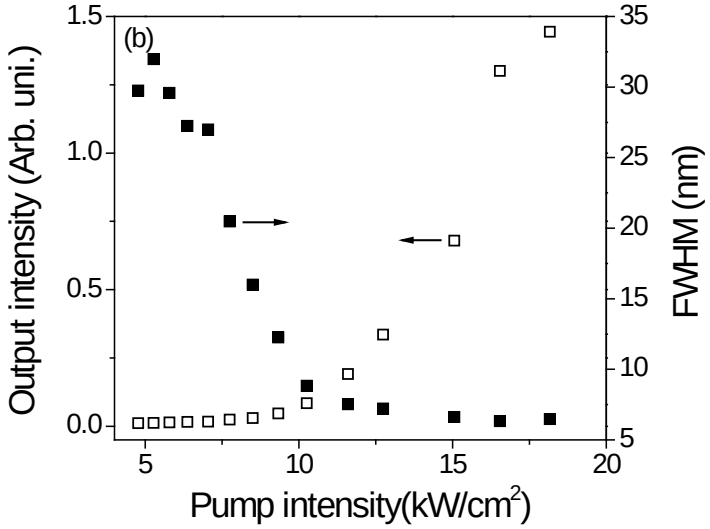

Figure 4. Emission spectra of DFB lasers based on 540 nm-thick films of mr-I7030E (a) and mr-I8030E (b), both resists doped with 1 wt% of PDI-O, obtained under excitation with different spot diameters (*D*).